The Periaxonal Space of Crayfish Giant Axons

PETER SHRAGER, JOHN C. STARKUS, MEI-VEN C. LO, and CAMILLO PERACCHIA

From the Department of Physiology, University of Rochester Medical Center, Rochester, New York 14642

ABSTRACT The influence of the glial cell layer on effective external ion concentrations has been studied in crayfish giant axons. Excess K ions accumulate in the periaxonal space during outward K^+ current flow, but at a rate far below that expected from the total ionic flux and the measured thickness of the space. At the conclusion of outward current flow, the external K^+ concentration returns to normal in an exponential fashion, with a time constant of ~2 ms. This process is about 25 times faster than is the case in squid axons. K^+ repolarization (tail) currents are generally biphasic at potentials below about −40 mV and pass through a maximum before approaching a final asymptotic level. The initial rapid phase may in part reflect depletion of excess K^+. After block of inactivation and reversal of the Na^+ concentration gradient, we could demonstrate accumulation and washout of excess Na ions in the periaxonal space. Characteristics of these processes appeared similar to those of K^+. Crayfish glial cell ultrastructure has been examined both in thin sections and after freeze fracture. Layers of connective tissue and extracellular fluid alternate with thin layers of glial cytoplasm. A membranous tubular lattice, spanning the innermost glial layers, may provide a pathway allowing rapid diffusion of excess ions from the axon surface.

INTRODUCTION

The repolarization of the axon membrane during an action potential depends upon a passive efflux of potassium ions of the order of a few picomoles per square centimeter per impulse. Membranes of axons and surrounding glia are separated by a thin region (100–300 Å), the periaxonal space, into which extend the oligo- and polysaccharide chains of membrane glycoproteins and glycolipids. This space, which constitutes the immediate extracellular environment of the neuron, communicates

Address reprint requests to Dr. Peter Shrager, Dept. of Physiology, Box 642, University of Rochester Medical Center, 601 Elmwood Ave., Rochester, NY 14642. Dr. Starkus' present address is Pacific Biomedical Research Center, University of Hawaii at Manoa, Honolulu, HI 96822.

J. GEN. PHYSIOL. © The Rockefeller University Press · 0022-1295/83/08/0221/24 $1.00

Volume 82 August 1983 221–244

with "bulk" extracellular fluid via clefts between glial cells and possibly through other more highly specialized structures. Since the normal periaxonal K^+ concentration, $[K^+]_o$, is just a few millimolar, and the above morphology limits diffusion from the periaxonal space, significant increases in $[K^+]_o$ may arise during repetitive activity. The resting depolarization that results can, in turn, influence further excitation.

The variation of $[K^+]_o$ with axon activity was first described by Frankenhaeuser and Hodgkin (1956). In experiments on squid axons they found that during a train of impulses at 125 Hz, $[K^+]_o$ rose by 17 mM in 300 ms. Excess K^+ then disappeared in an exponential fashion with a time constant of 30–100 ms. K^+ accumulation has been characterized further, both in giant axons and in myelinated fibers, by a number of workers, including Binstock and Goldman (1971), Adelman et al. (1973), Adam (1973), Dubois and Bergman (1975), Taylor et al. (1980), Moran et al. (1980), and Dubois (1981*a*). The physiological and pathological consequences of K^+ accumulation have been the subject of several recent symposia and reviews (Varon and Somjen, 1979; Orkand, 1979; Nicholson, 1980; Gardner-Medwin, 1981).

We have been interested in the characteristics of periaxonal ion accumulation in giant axons of the crayfish for a number of reasons. First, excess ions disappear with kinetics much faster than those of other preparations and may reflect a highly specialized relationship between axons and glia. Second, an accurate description of K^+ accumulation is essential to any attempt at measuring and modeling K^+ channel gating kinetics. Finally, we wished to compare periaxonal handling of K^+ with that of Na^+ in order to judge the relative distributions of K^+ and Na^+ channels in the axon membrane. We report here the results of electrophysiological experiments and attempt to correlate our findings with morphological information.

METHODS

Medial giant axons of the crayfish *Procambarus clarkii* were dissected and voltage-clamped with an axial wire system as described in detail previously (Shrager, 1974; Starkus and Shrager, 1978; Lo and Shrager, 1981). Pulse generation and data analysis were accomplished using a minicomputer (PDP 8/A-620; Digital Equipment Corp., Maynard, MA). In some experiments, fibers were internally perfused after insertion of a second pipette (Shrager, 1975; Starkus and Shrager, 1978). The standard external medium was that of Van Harreveld (1936) (NVH) and contained (mM): 205 NaCl; 5.4 KCl; 2.6 $MgCl_2$; 13.5 $CaCl_2$; 2.3 $NaHCO_3$; pH 7.5–7.6. In many of these experiments the K^+ concentration was raised or lowered by substituting Na^+ 1:1. These solutions are called K*x*VH, where *x* is the K^+ concentration in millimolar. Other salts were unchanged. In experiments involving changes in $[Cl^-]_o$ or temperature, 2 mM Hepes buffer was added, with the pH adjusted for the temperature used. Other external solutions used are given in the text. The standard internal perfusate (P1) contained (mM): 109 KF; 37 K_3 citrate; 15 NaCl; 93 mannitol; pH 7.35. Other internal solutions are listed in the text. Where noted, tetrodotoxin (TTX) was added externally to block Na^+ channels. In all K^+ accumulation experiments, the holding potential was

kept within 1–2 mV of the resting potential to avoid loading or unloading of the periaxonal space by the holding current. In the experiments on Na^+ accumulation the membrane was held at 5–35 mV hyperpolarized from the resting potential. The inward holding current would tend to deplete the periaxonal space of Na^+, but since the latter was just 2.3 mM in the bulk medium, even a reduction to zero would constitute only a small change in $[Na^+]_o$.

A rough subtraction of capacitative transients was made during experiments using an electronic analog. Final subtraction was done later using either reciprocal pulses or a divided-pulse procedure (Bezanilla and Armstrong, 1977). This latter scheme, a P/3 pattern, was adopted to avoid K^+ currents during the pulses used for subtraction of capacitative transients from K^+ tail currents. K^+ tail currents were elicited by depolarizing the axon to open K^+ channels and then returning V_m to the desired value. After this set of pulses (set A) the fiber was hyperpolarized and a set of pulses of one-third the magnitude of set A was applied (set B). Set B was designed so that V_m was never more positive than −78 mV and hence never in the range of K^+ channel activation. One A set and three B sets were summed by the computer. The process was sometimes repeated once to improve the signal-to-noise ratio.

Leak currents were subtracted assuming that leakage conductance was linear and had a reversal potential equal to the resting potential. This correction was in general very small and had little effect on measured reversal potentials. It was significant only in determining the positive phase of tail currents, as will be discussed later. "Instantaneous" values of tail currents were measured at 60 or 62.5 μs (depending on sampling rate) after the start of repolarization.

Histology: Thin Sections

Crayfish ventral nerve cords were fixed in 3–6% glutaraldehyde followed by 2% osmium tetroxide, each buffered to pH 7.4. Samples were dehydrated and embedded in Epon or Araldite. Sections were cut on an LKB Ultratome microtome (LKB Instruments, Inc., Gaithersburg, MD) to a thickness of ~50 nm. They were observed with an AEI EM 6B electron microscope after staining with uranyl and lead salts. Further details are given in Peracchia and Robertson (1971).

Histology: Freeze Fracture

Crayfish ventral nerve cords were fixed in buffered 3–6% glutaraldehyde-H_2O_2 and placed in a series of glycerol solutions (5, 10, 20, and 30%) at 4°C. Interganglionic portions were cut into 1-mm segments and were rapidly frozen in liquid Freon 22 at −150°C. The segments were fractured longitudinally at −110°C with a Denton freeze-fracture device (Denton Vacuum Inc., Cherry Hill, NJ). Samples were shadowed with carbon-platinum at 45°, and carbon at 90°. Replicas were coated with collodion and specimens were digested in chlorox. The collodion was dissolved in amyl acetate and samples were observed with an AEI EM 801 electron microscope. Further details are given in Peracchia (1974).

RESULTS

Potassium Accumulation in the Periaxonal Space

The potassium concentration just external to K^+ channels increases with a maintained outward K^+ current. In Fig. 1 we have superimposed K^+

currents of three different durations. The membrane potential was stepped from −76 to +35 mV for 2, 4, or 6 ms, and then returned to −76 mV. Early K^+ repolarization (tail) currents grew increasingly negative as the pulse duration was increased. Since the K^+ concentration in the bulk external medium was 2.7 mM and that in the axoplasm was ~247 mM (Wallin, 1966), the zero current (reversal) potential for the highly selective K^+ channel (Hille, 1973) should be well negative to −76 mV, and we would expect tail currents in the absence of periaxonal ion accumulation to be outward in this experiment. We found that K^+ tail currents could be reasonably well fitted by the sum of two exponential functions and under some conditions included a delayed outward phase.

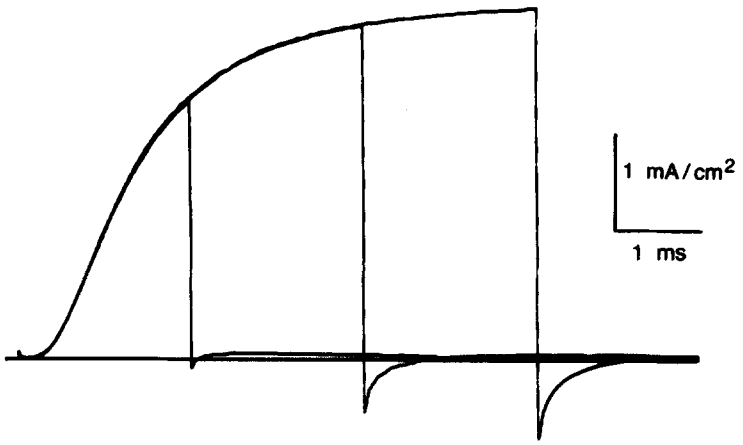

FIGURE 1. K^+ accumulation in the periaxonal space. Superposition of three K^+ currents of 2, 4, and 6 ms duration. Holding potential, −76 mV. Pulses to +35 mV were followed by a return to −76 mV. Records were taken first in (mM): 207.7 NaCl; 2.7 KCl; 2.6 $MgCl_2$; 13.5 $CaCl_2$; 2.3 Hepes; 100 nM TTX; pH 7.6. Pulses were repeated after addition of 2 mM 4-aminopyridine. The currents shown are results after subtraction of traces in 4-aminopyridine.

We consider first whether these repolarization currents are a proper record of potassium flows.

In much of this work we shall use "instantaneous" current-voltage curves (see Methods) to derive reversal potentials which, in turn, will be used to calculate periaxonal ion concentrations. As one test for the adequacy of this procedure we ran experiments at two different K^+ concentrations in the external medium. After a depolarizing prepulse to activate K^+ conductance, V_m was returned to different levels, allowing construction of instantaneous *I-V* curves from tail currents. The prepulse duration was held to 3 ms to minimize loading of the periaxonal space. Measurements were made at bulk K^+ concentrations of 5.3 and 15.0 mM, which represented a shift in the K^+ equilibrium potential of ~25 mV.

Prepulse amplitudes were designed to keep the total K^+ efflux (integrated K^+ current) equal at the two concentrations. We calculated first the periaxonal $[K^+]_o$ after the prepulse in K^+ 5.3 mM medium. Subtracting 5.3 mM gave the increment in $[K^+]_o$ because of loading by the prepulse (12–16 mM). Since loading was designed to be constant, we added this increment to 15 mM, which then allowed calculation of a predicted reversal potential for tail currents in the 15 mM K^+ medium. In one axon the measured value was within 5 mV of the predicted number, and in another the difference was <1 mV.

As further evidence that these tail currents represent K^+ ions moving through K^+ channels, we added 4-aminopyridine, which blocks K^+ channels with no effect on Na^+ channels (Meves and Pichon, 1975; Yeh et al., 1976) and we repeated the pulse protocols. All phases of K^+ tail currents were absent in 4-aminopyridine and the records of Fig. 1 represent results after subtraction of sweeps with the blocking drug present. As will be noted below, we also did experiments on perfused axons, using tetraethylammonium ion (TEA^+) as a K^+ channel blocker (Armstrong and Binstock, 1965), again with results consistent with tails representing K^+ currents. Finally, the shape of these repolarization currents was also sensitive to the bulk external $[K^+]$, as will be discussed later (Fig. 7).

Fig. 2 illustrates instantaneous *I-V* curves for an axon after two different depolarizations. In the first case (open circles) a pulse to +58 mV was applied for 2 ms and V_m was then stepped to various levels, given on the abscissa. The ordinate represents the current recorded 62.5 μs after the end of the 2-ms pulse. The P/3 procedure has been used to subtract the capacitative transient. The reversal potential following this short pulse was −95 mV. When the pulse duration was increased to 18 ms, the reversal potential was shifted to −59 mV (Fig. 2, filled circles). Since the K^+ channel has a very high selectivity for K ions (Hille, 1973), we used the Nernst equation to calculate $[K^+]_o$ at the conclusion of the loading pulse as 5 mM for the 2-ms pulse and 22 mM for the 18-ms pulse. The K^+ concentration in the external bath was 2.7 mM.

Integrating the K^+ current during the 2-ms loading pulse shows that 26 pmol K^+/cm^2 left the fiber. We measured the thickness of the space between the axon and the Schwann cell membranes in this preparation from electron micrographs as ~150 Å. Allowing for some shrinkage during fixation, we shall use 200 Å as a nominal figure. If all the K^+ accumulated in the periaxonal space during the pulse, the increment in $[K^+]_o$ should have been 13 mM and the total $[K^+]_o$ 15.7 mM, about three times the measured value. Relatively little K^+ would leave the space because of current flow since the transport number for external K^+ is at most 0.03. Thus, ~10 mM K^+ left the periaxonal space via some other process during the 2-ms pulse. A similar calculation for the 18-ms depolarization shows that 797 pmol K^+/cm^2 entered the periaxonal space, which represented an increment of 386 mM over and above that of the 2-ms pulse. The measured increment, however, was 22 − 5 = 17 mM.

369 mM K^+ or 96% of the efflux left the periaxonal space over a 16-ms period. In another example, the expected increment between 3- and 8-ms pulses was 73 mM K^+, while the measured value was only 6 mM. These results are in contrast with those of squid axons in which the measured $[K^+]_o$ is close to that expected from the total K^+ flow (Frankenhaeuser and Hodgkin, 1956).

The instantaneous *I-V* curves of Fig. 2 are not linear. The ×'s represent an attempt to fit the data using the constant-field current equation (Goldman, 1943; Hodgkin and Katz, 1949). The fit seems adequate at all

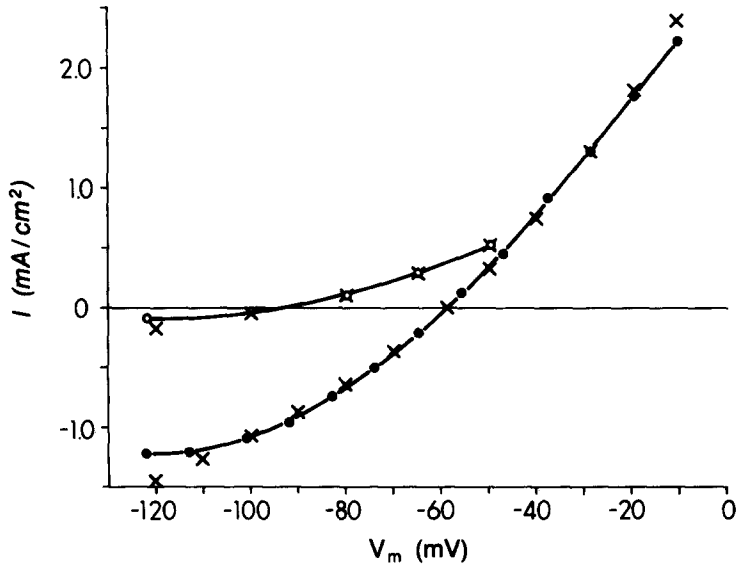

FIGURE 2. Instantaneous K^+ current-voltage curves. Currents (ordinate) were measured 62.5 μs after changing V_m from the prepulse level of +58 mV to the value given on the abscissa. Circles represent experimental data. Prepulse duration: open circles, 2 ms; solid circles, 18 ms. Lines were drawn by eye to connect the circles and have no theoretical significance. ×'s show fits of the Goldman-Hodgkin-Katz constant field current equation with $[K^+]_i$ = 234 mM and $[K^+]_o$ = 5.2 mM (2 ms prepulse) or 20.7 mM (18 ms prepulse). Intact axon. External solution, K2.7VH; TTX, 100 nM. Holding potential, −80 mV.

but the most negative potentials, where it does not provide sufficient rectification.

We have studied the rate of disappearance of excess K^+ ions from the periaxonal space in more detail. In these experiments a strong depolarization was first applied to elicit large outward K^+ currents and load the space (see inset to Fig. 3*A*). V_m was then returned to a potential at or near the holding potential for a variable period, *T*. The potential during time *T* was chosen to minimize loss or gain of K^+ caused by tail currents at the conclusion of the loading pulse. After period *T*, a brief and small depo-

larization just sufficient to open a significant fraction of K^+ channels was applied and followed, as in the experiment of Fig. 2, by steps to various potentials. A complete set of steps was applied for each T, allowing construction of instantaneous *I-V* curves and determination of reversal potentials. In this manner the time course of washout of K^+ could be followed directly. Results from these four-pulse experiments are shown in Fig. 3*A*. If we approximate the data by a single exponential function, excess $[K^+]_o$ left the periaxonal space with a time constant of ~2 ms. There were several difficulties that served to limit the accuracy of these measurements. One difficulty, tail currents at the beginning of period T, was mentioned above. Integrating these currents showed them to be a minor perturbation. Of greater importance was the K^+ current elicited during the short pulse after period T, which, although held to a minimum, nonetheless added a significant fraction of K^+ to the periaxonal space. Since the time course of this current was dependent on the K^+ conductance at the beginning of the pulse, and hence on T, this extra loading introduced a distortion in the measurement that could not be readily corrected. This was evident from the fact that $[K^+]_o$ never returned to the bulk external medium concentration, even at T values of several seconds. This persistent component, generally several millimolar in excess of $[K^+]_o$, was subtracted before graphing the results in Fig. 3*A* to allow normalization of the data from different axons. Even with this limitation, it seems clear that at least a large fraction of excess $[K^+]_o$ is washed out with very rapid kinetics.

From records of spike afterpotentials, Frankenhaeuser and Hodgkin (1956) found that accumulated K^+ left the periaxonal space of squid axons with a time constant of 30–100 ms. Since our results on crayfish fibers were significantly different, it was desirable to repeat our experimental procedure on squid nerve. We were fortunate to obtain a few axons of *Loligo pealei* from Dr. Ted Begenisich of this department. Our preparations were dissected from mantles that had been shipped to Rochester by air on ice and were used within a few hours of decapitation. The voltage-clamp system was identical to that used for crayfish axons, except that a 50-μm platinum wire was added to the internal electrode to allow for the higher total current. The results of experiments on two squid axons are shown as open symbols in Fig. 3*B*. The solid symbols, which are from crayfish axons, are repeated from Fig. 3*A* and are shown here on a compressed time scale for comparison. Although the squid data are limited, the time constant of washout was ~50 ms in each fiber, in good agreement with the results of Frankenhaeuser and Hodgkin (1956). Thus, the large difference between these preparations in the rate of removal of accumulated $[K^+]_o$ seems not to be dependent on the method of measurement used.

Sodium Accumulation in the Periaxonal Space

One aim of these experiments was to demonstrate the accumulation of

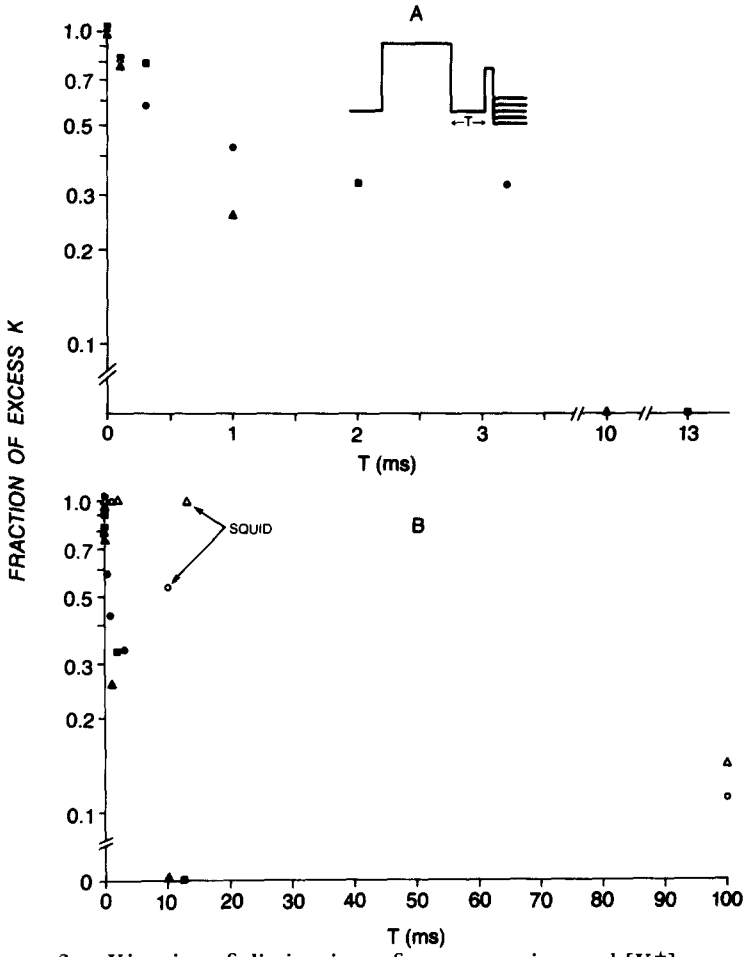

FIGURE 3. Kinetics of dissipation of excess periaxonal $[K^+]_o$ measured by the four-pulse technique. The pulse protocol used is shown in the inset and is described further in the text. For each value of T, instantaneous current-voltage curves were constructed from initial currents during the final pulse. $[K^+]_o$ was calculated from reversal potentials using the Nernst equation. (*A*) Intact crayfish axons were treated with external solution NVH (●) or K2.3VH (■); TTX, 0.1 μM for each. Inverse pulse patterns were applied to allow substraction of linear capacitative and leakage currents. The symbol ▲ represents a perfused crayfish axon with internal solution (mM): 109 KF; 37 K_3 citrate; 15 KCl; 93 mannitol; pH 7.35; and external solution (mM): 210.4 tetramethylammonium Cl; 2.6 $MgCl_2$; 13.5 $CaCl_2$; 2.3 $KHCO_3$; 100 nM TTX; pH 7.6. Capacitative currents were removed by repeating all pulses after adding 15 mM tetraethylammonium Cl internally to block K^+ currents, and subtracting the resulting records. Other details are given in the text. (*B*) Solid symbols are as in *A*. Open symbols represent intact squid axons in artificial seawater containing (mM): 440 NaCl; 50 $MgCl_2$; 10 $CaCl_2$; 5 Hepes; 150 nM TTX; pH 7.5. In one axon (△), 2.3 mM KCl was added externally. Capacitative and leakage currents were removed using reciprocal pulses.

Na^+ in the periaxonal space and to compare quantitatively the loading and washout kinetics of Na^+ with those of K^+ as a means of judging possible differences in the distribution of Na^+ and K^+ channels in the axon membrane. As will be seen, we have to date been only partially successful in achieving this goal. Na^+ accumulation is normally not detected in voltage-clamp experiments because the bulk external Na^+ concentration is high and because Na^+ currents inactivate. The first condition is readily circumvented by reversal of the sodium concentration gradient in internally perfused axons. Removal of Na^+ channel inactivation requires chemical modification. Pronase, a mixture of proteolytic enzymes that achieves this goal in squid axons (Armstrong et al., 1973), is more difficult to use in crayfish fibers (Starkus and Shrager, 1978). From

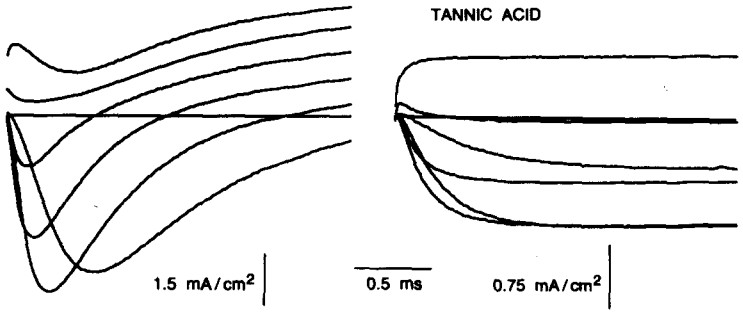

FIGURE 4. Block of Na^+ channel inactivation by tannic acid. Left, control currents. Right, after a 10-min exposure to 40 μM tannic acid added internally. External solution, NVH; internal solution, P1. Depolarizations from a holding potential of −68 mV to −28, −8, 12, 32, 52, and 72 mV. Temperature, 8°C.

records of action potentials and membrane impedance changes, Shrager et al. (1969) concluded that internal perfusion of crayfish axons with tannic acid greatly prolonged the increase in sodium conductance during a depolarization. Under voltage clamp, tannic acid has been shown to prevent Na^+ channel inactivation in crayfish (Shrager and Starkus, 1979) and squid (Horn et al., 1980) axons.

In Fig. 4 we show families of ionic currents recorded in a perfused crayfish axon before (left) and after (right) the addition of 40 μM tannic acid to the internal perfusate. This experiment was done with a normal Na^+ concentration gradient. K^+ currents are virtually eliminated, as is Na^+ channel inactivation. The remaining Na^+ currents are reduced in amplitude and activation is slowed. The action of tannic acid is irreversible on washing, and the reagent was generally applied at levels of 10–30 μM for ~10 min and was then removed. Fig. 5 gives records from an experiment designed to measure steady state inactivation. Sweeps on the left are controls and those on the right follow a brief exposure to tannic acid. The fiber was held at −74 mV, and test pulses to +6 mV were preceded by 50-ms prepulses to −74, −69, −64, −59, or −54 mV. In this experiment the reagent was withdrawn before removal of inactivation

was complete. A depolarization to +6 mV with no prepulse (Fig. 5, largest peak current on the right) then elicited a Na^+ current that partially inactivated before reaching a steady state level. Depolarizing prepulses affected only the component of the Na^+ current that inactivated, and the voltage dependence of the decline of this component was similar to that of control currents (Fig. 5, left). The results of Figs. 4 and 5 suggest that during exposure to tannic acid an increasing number of Na^+ channels become modified over time. Modified Na^+ channels no longer inactivate, whereas unreacted channels behave normally. Tannic acid thus seems to act by direct reaction with Na^+ channels rather than by a more general and nonspecific interaction with membrane components, which might lead to a heterogeneous population of Na channels of various degrees of modification.

For experiments on Na^+ loading of the periaxonal space, internally

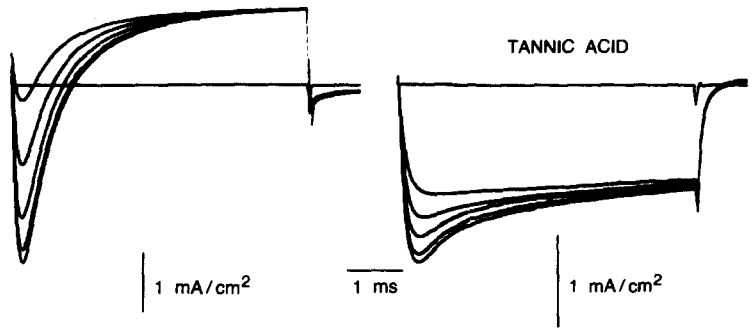

FIGURE 5. Steady state Na^+ channel inactivation with tannic acid. Left, control records. Right, after a 10-min exposure to 30 μM tannic acid. Holding potential, −74 mV. Test pulses to +6 mV were preceded by 50-ms prepulses to −74, −69, −64, −59, or −54 mV. External solution, NVH; internal solution, P1. Temperature, 8°C.

perfused crayfish axons were exposed to tannic acid for a brief period as above and the Na^+ concentration gradient was reversed. Low external $[Na^+]_o$ was achieved by substitution with tetramethylammonium ion. Internally, Na^+ was substituted for K^+. Solutions were designed so that concentration gradients were identical when measuring either K^+ or Na^+ loading. In addition, it was necessary to attempt to match steady state outward currents in the two experiments. Fig. 6 shows results from a pair of fibers in which all conditions were met. Loading depolarizations of four different durations were followed by a return to various potentials to allow construction of instantaneous *I-V* curves and determination of reversal potentials. Calculated concentrations in the periaxonal space are plotted vs. the integrated loading current. The steady state current was ~2 mA/cm² in each case. Considering the range of uncertainty in our measurements, we find no significant difference between the two curves. Loading of the periaxonal space appears to be the same for Na ions

moving through Na^+ channels as for K ions moving through K^+ channels. As was the case for K^+, the $[Na^+]_o$ expected from integrating the loading current was severalfold larger than the measured value. This is partially reflected in the apparent saturation of these curves. We have attempted

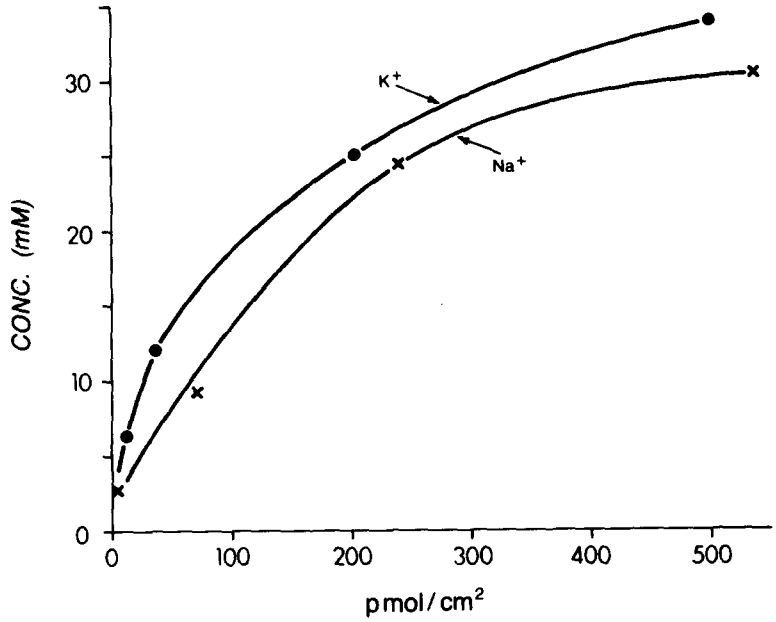

FIGURE 6. Loading of the periaxonal space by K^+ or Na^+. Depolarizing pulses elicited outward ionic currents to load the periaxonal space. They were followed by voltage steps that allowed construction of instantaneous current-voltage curves. Concentrations were then calculated from the zero-current potentials using the Nernst equation. The duration of the initial depolarizing pulse was varied to change the degree of loading. The current during this pulse was integrated by the computer and is plotted on the abscissa. In the Na^+ experiment the axon was exposed to 30 μM tannic acid for 10 min to remove inactivation. Solutions for the Na^+ experiment were: external (mM): 210.4 tetramethylammonium Cl; 2.6 $MgCl_2$; 13.5 $CaCl_2$; 2.3 $NaHCO_3$; pH 7.6; and internal (mM): 109 NaF; 37 Na_3 citrate; 15 NaCl; 93 mannitol; pH 7.35. Capacitative and leakage currents were removed by subtracting records with 100 nM TTX added externally. Solutions for the K^+ experiment were identical, except that K^+ replaced Na^+ both internally and externally. Capacitative and leakage currents were removed using reciprocal pulses. 100 nM TTX was present externally. Lines were drawn by eye to indicate trends. Temperature, 8°C.

further to measure washout of Na ions after loading, in four-pulse experiments similar to those described earlier for K^+. This proved to be difficult. The protocol required that properties of the axon be stable for a long period, with numerous substantial prolonged depolarizations. Axons treated with tannic acid generally had an accelerated rate of

decline. Further, the problem of the failure of the measured periaxonal concentration to return to the bulk level even after long washout times was more severe in the case of Na^+. We were able to complete protocols in just two fibers. Both had a rapid component of washout, with a time constant of ~2 ms. This value is similar to that measured for $[K^+]_o$, but must be regarded as preliminary because of the above difficulties.

Potassium Tail Currents

If K ions leave the periaxonal space with the rapid kinetics described above, then this change in driving force should be reflected in K^+ tail currents. We noted earlier that these currents were characterized by two time constants and, in ~80% of axons, included a reversal of direction at certain potentials. We tested whether these properties were an artifact caused by polarization of the current electrode during the loading pulse. This seemed unlikely because (*a*) the shape was similar even when the loading pulse was very short, as can be seen in Fig. 1; (*b*) during maintained depolarizations, K^+ currents reached a flat steady state level at all potentials and at both high and low current densities, even out to 18 ms, the longest duration used in these studies; (*c*) the positive phase of the tail currents is in the wrong direction to be accounted for by polarization. Since we suspected that the tail current kinetics might be related to events in the periaxonal space, we examined them in elevated bulk external $[K^+]$. Fig. 7 illustrates records in media with $[K^+]$ equal to 5.3 and 15 mM. The depolarizing prepulses were kept relatively short and were matched to keep total K^+ flux equal. The positive phase disappeared in the elevated $[K^+]$ medium. The curve at 15 mM K cannot be reproduced by simply shifting the current at 5.3 mM K downward. The latter passes through a maximum (seen more clearly on a compressed time base), whereas the former does not. Finally, we noted earlier (Fig. 1) that the tail current shape is unaltered by subtraction of records in 4-aminopyridine. We therefore proceeded to examine K^+ tail current kinetics in more detail.

A family of K^+ tail currents at six different potentials following a prepulse depolarization is shown in Fig. 8. The P/3 procedure has been used to subtract the linear capacitative current and a small correction for leakage current has been made. The zero-current level is shown for each record. Tail currents have been analyzed by fitting the sum of two exponential functions to them. The slower component (τ_2) was fitted first, the calculated curve was subtracted, and the faster component (τ_1) was matched. The calculated curves have been superimposed with the measured currents in Fig. 8 and the fit is satisfactory. Data from several axons at 10°C are plotted vs. membrane potential in Fig. 9. The open symbols represent τ_1; the solid symbols represent τ_2. τ_1 ranged between 0.2 and 0.4 ms among different axons, with a fair degree of scatter at each V_m. If the points are averaged in clusters of two to five and plotted at their voltage midpoints, it can be seen that in the range −125 to −80 mV, τ_1

increases by ~50%, as does τ_2, whereas at more positive potentials τ_1 is relatively independent of voltage. τ_1 at −40 to −50 mV is just 16% lower than τ_1 at −65 and to −75 mV. τ_2, which was an order of magnitude larger, had a peak value near −65 mV and displayed a sharp decrease at depolarized levels. Within the range −20 to −60 mV, K^+ currents elicited during a test depolarization are small and are accompanied by only minimal loading of the periaxonal space. We fitted the Hodgkin and Huxley (1952) kinetic scheme to these currents. In this model, the dependence of K^+ conductance on V_m and time is expressed through the

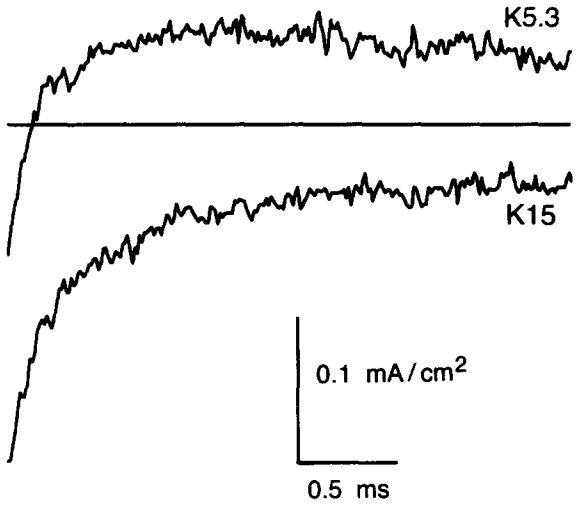

FIGURE 7. Dependence of K^+ tail currents on external [K^+]. K^+ tail currents recorded using the P/3 procedure after a 3-ms prepulse. K5.3 external solution contained (mM): 205.1 NaCl; 5.3 KCl; 13.5 $CaCl_2$; 2.6 $MgCl_2$; 2.3 Hepes; 100 nM TTX; pH 7.6. K15 external solution contained (mM): 195.4 NaCl; 15.0 KCl; other salts were as in K5.3 medium. Holding potential, −72 mV (K5.3); −56 mV (K15). 3-ms prepulses to +27 mV (K5.3); +52 mV (K15), then repolarization to −69 mV (K 5.3); −68 mV (K15). Prepulse levels were chosen to keep K^+ accumulation the same in each solution. Intact axon, 9.5°C.

fourth power of a probability variable, n, which obeys first-order kinetics. These fits were only marginally adequate. The values of τ_n obtained are plotted as the half-filled symbols in Fig. 9. Both the magnitude and the voltage dependence of τ_n are similar to those of τ_2 measured from tail currents.

As further tests of the mechanisms responsible for K^+ tail currents, we measured the temperature dependence of each time constant. Records were compared at 6.5 and 16.5°C. The Q_{10} for τ_1 was 1.3 (range 0.89–1.75), and that for τ_2 was ~2. In the same axons the Q_{10} for τ_n, measured from K^+ currents as described above, was 3.2. The possible contribution of active transport via the Na^+-K^+ ATP-driven pump in removal of excess

periaxonal K^+ was tested by the addition of 0.5 mM ouabain to the external bath of axons at 16.5°C. The biphasic nature of the K^+ tail currents was preserved. τ_1 was increased by ~20% in the presence of ouabain.

Glial Cell Structure

We have studied the ultrastructure of the glial cell sheath of crayfish axons in detail and have found it to differ significantly from that of squid giant axons (Geren and Schmitt, 1954; Villegas and Villegas, 1960;

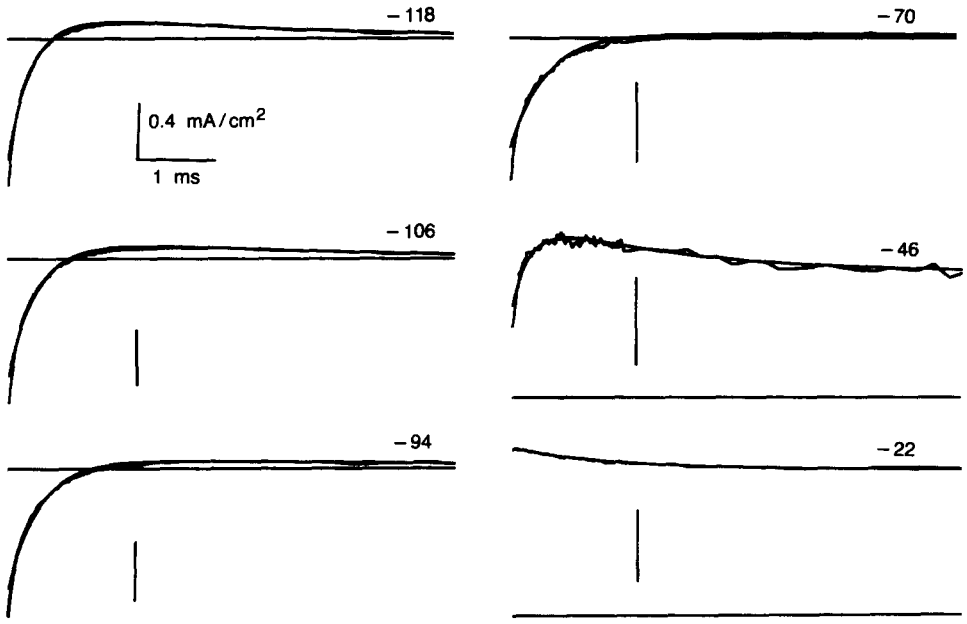

FIGURE 8. Family of K^+ tail currents. A 10-ms prepulse to +65 mV preceded these records. V_m for each current is given in the figure. P/3 procedure. Intact axon. External solution K4.0VH; 100 nM TTX. Holding potential, −76 mV. The sum of two exponential functions was fitted to the data (see Fig. 9) and is shown superimposed for each trace. Temperature, 9.5°C. The vertical bar indicates 0.4 mA/cm^2. The scale applies to all records.

Villegas, 1969). In crayfish fibers the Schwann cell sheaths consist of layers of glial cell cytoplasm alternating with spaces containing extracellular fluid and connective tissue (Peracchia and Robertson, 1971; Ballinger and Bittner, 1980). Electron micrographs of thin sections are shown in Fig. 10. The layer adjacent to the axon contains glial cytoplasm and ranges in thickness from 0.2 to 1 μm. The periaxonal space is visible at high magnification (Fig. 10*b* and 10*c*) as the clear region separating the axon and the Schwann cell membranes. The tortuous clefts separating adjacent Schwann cells are much less prominent than in the case of squid

fibers. Crayfish glial cells, however, contain patches of membranous tubular lattices (Peracchia and Robertson, 1971), visible in several regions in Fig. 10*a* (arrows). The inset to Fig. 10*a*, which is from another fiber, shows this tubular network more clearly. At one point (arrow) a tubule is seen opening into the periaxonal space. This communication is seen in detail in Figs. 10*b* and *c*, which are from two other axons. In Fig. 10*c* an "h"-shaped tubule is seen to link the periaxonal space with the first band of extracellular fluid and connective tissue. The glial tubules are ~400

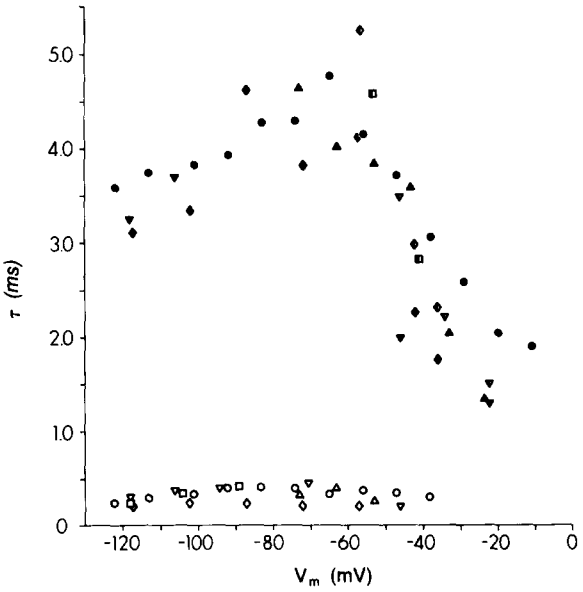

FIGURE 9. Kinetics of K^+ tail currents. The slow component of each tail current was fitted first by a single exponential function (τ_2). After subtraction of this component the faster phase was fitted in similar fashion (τ_1). Solid symbols represent τ_2; open symbols represent τ_1. K^+ currents during several test depolarizations were recorded and analyzed using Hodgkin-Huxley (1952) n^4 kinetics. Resulting values of τ_n are plotted as half-filled symbols. External solution K2.7VH (○, □, ◇), K4VH (▽), K5.4VH (△; 100 nM TTX. Temperature, 9.5°C.

Å in diameter. At points of interconnection within the lattice, tubules form enlarged cavities ~500 Å in diameter (Fig. 10).

The tubular system is visible also after freeze fracture (Fig. 11). The top surface of the schematic diagram illustrates the fracture plane. Beginning at the upper right of the micrograph the figure illustrates the axoplasm (A), containing several mitochondria; the protoplasmic face of the axon surface membrane (P_{AX}); the exoplasmic face of the adaxonal Schwann cell membrane (E_{SC}), containing numerous tubule openings (upward arrowheads); the Schwann cell cytoplasm (SC); and the proto-

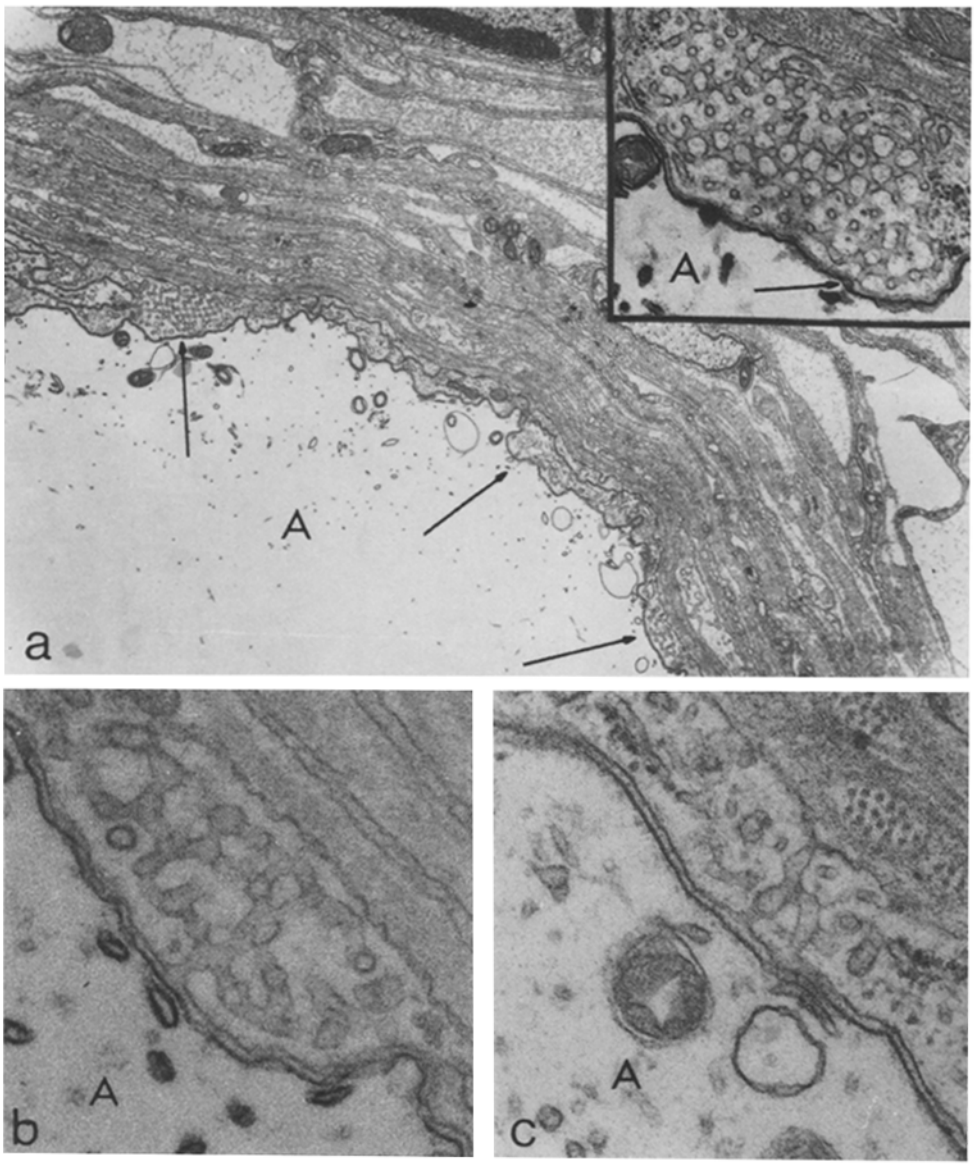

FIGURE 10. Electron micrographs of thin sections of crayfish axons. All show axon (axoplasm = A) and surrounding glial connective tissue sheath. (*a*) Several regions of glial cytoplasm containing tubular elements are visible (arrows). Note the striated appearance of alternating layers of Schwann cell cytoplasm (light bands) and connective tissue (darker bands). × 13,500. Inset (different fiber) shows the tubular lattice in more detail. Arrow indicates opening of a tubule into the periaxonal space. × 28,000. (*b*, *c*) Enlarged views of the tubular system showing openings to the periaxonal space (*b*, *c*) and to the adjacent extracellular fluid-connective tissue layer (*c*). × 60,000.

plasmic face of the outer Schwann cell membrane (P_{SC}), in which some tubule openings are also visible (downward arrowheads). In the lower left corner a small region of the adjacent connective tissue layer (C) is illustrated. The periaxonal space is seen as the border between the P_{AX} and E_{SC} faces. At one point (arrows) a single tubule is seen traversing the entire Schwann cell cytoplasmic layer. Within the patch of E_{SC} visible, the average spacing between tubule openings into the periaxonal space is ~ 0.2 μm. The projections (P) of the axolemma (and adaxonal glia) into the axoplasm have been described in detail by Peracchia (1974).

DISCUSSION

Two lines of evidence suggest that excess K ions in the periaxonal space of crayfish fibers are removed with a time constant of the order of 1 ms. First, most of the total K^+ moved into the periaxonal region during a depolarization of a few milliseconds is effectively dissipated by the end of the pulse. Second, our four-pulse technique allowed a more direct measure of washout kinetics and suggested a time constant of ~ 2 ms. Although they are not as complete as those for K^+, our results suggest that Na ions that move through Na^+ channels into the periaxonal space share a similar rapid dissipation. The fiber in this case has been modified by tannic acid, a large polyphenol that binds and cross-links proteins. With regard to the axon membrane, our analysis of steady state inactivation shows that effects of the compound on Na^+ conductance result from a direct interaction with Na^+ channels. Tannic acid (1,701 mol wt) is not likely to be permeant through the axolemma. It was applied only internally, at a maximum concentration of 40 μM, and exposure was limited to 10 min. It is thus highly unlikely that the periaxonal region was modified by this compound. Although we did not detect any major difference between K^+ and Na^+ in loading and washout kinetics, this method is not sufficiently sensitive to detect differences in channel distributions over distances of less than ~ 1 μm.

We now consider several characteristics of measured K^+ tail currents. The simplest mechanism for the biphasic tail currents observed in external media of low $[K^+]$ would involve first a loading of the periaxonal space by K^+ during the preceding depolarization. The fast initial decrease in tail current would then result from a rapid washout of accumulated K^+. If the K^+ equilibrium potential, V_K, fell below V_m, the K^+ current would become outward. The slower, final decline of K^+ tails might then reflect a closing of K^+ channel gates to a new steady state distribution corresponding to the new V_m. This interpretation is supported by the behavior of K^+ tail currents in media of higher $[K^+]$. On the other hand, the kinetics of the initial phase (τ_1) are significantly faster than those measured for K^+ washout by the four-pulse experiments. However, the latter is not accurate at very short times because the pertubations of the short activating pulse are most pronounced here. The positive phase of tail currents persisted

even at the most negative V_m tested (−122 mV) and its reversal potential thus seems to be negative to V_K. One important difficulty concerns the correction used for leakage conductance, g_l. Our treatment of the data

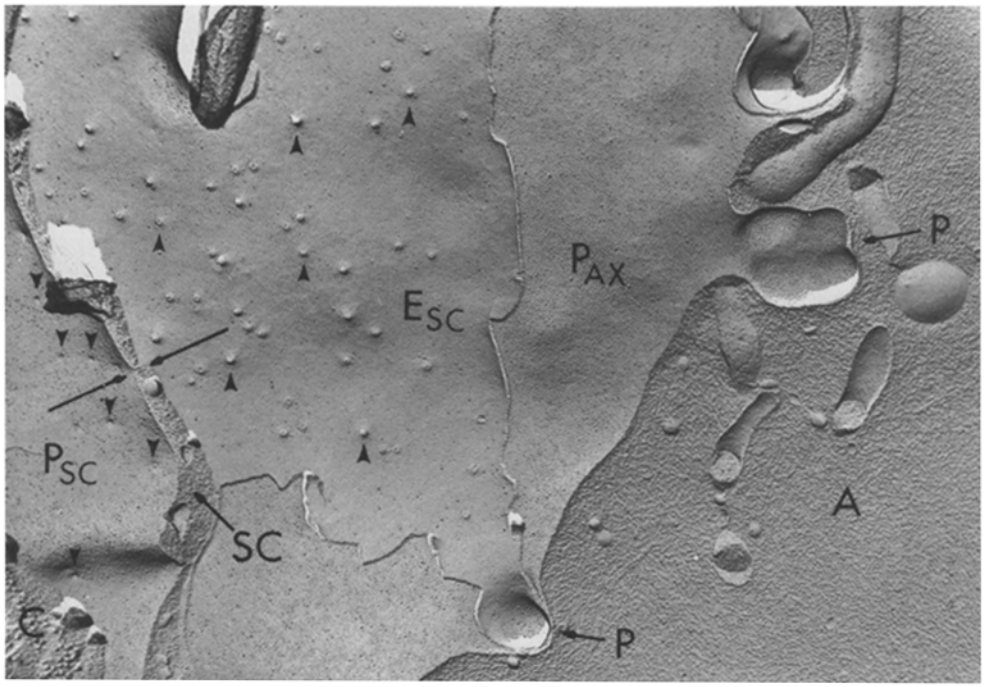

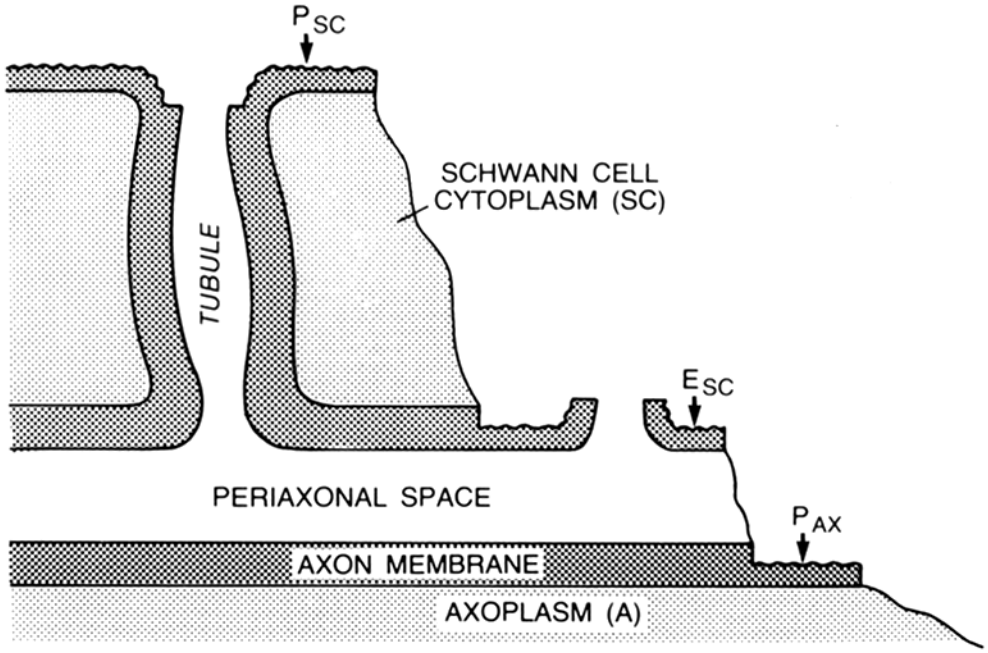

assumed that g_l was linear and time independent. The latter may not be true since the $[K^+]_o$ is changing during the first 1–2 ms after repolarization. A very small (40 $\mu A/cm^2$), time-dependent component in set B currents, examined in one axon, was sufficient to reduce the "overshoot" in tail current to zero when included in the leakage correction. In the mammalian central nervous system, extracellular K^+ measured with K^+-sensitive electrodes undershoots the nominal bulk value after cessation of a high-frequency burst (Kriz et al., 1975). This would probably have only a small effect on the outward phase of tail currents in our experiments, since, in the constant-field formulation, K^+ current becomes relatively insensitive to $[K^+]_o$ at low concentrations. Orkand et al. (1966) have suggested a "spatial buffering" of excess perineural $[K^+]_o$ by glia in which K^+ enters glial cells in regions of high $[K^+]_o$ and leaves in areas more distal to the neuron. This mechanism, which could contribute to a rapid removal of excess K^+, would also generate local currents that could distort voltage-clamp records in a manner similar to that of series resistance. Alternatively, biphasic K^+ tail currents may reflect activation of another ionic channel. Dubois (1981*a*, *b*) has shown that in frog node of Ranvier K^+ current tails may reflect both dissipation of accumulated K^+ and gating kinetics. He further found a very slow component in these currents that is most prominent after depolarizations lasting hundreds of milliseconds. We have not examined this latter point.

It is of interest to attempt to correlate the characteristics of ion accumulation in the periaxonal space with glial cell ultrastructure, and to compare our results on crayfish fibers with those of other unmyelinated axons. Binstock and Goldman (1971) found very little K^+ loading in *Myxicola* axons and attributed this to an effective thickness of the periaxonal space of 2,240 Å. However, they report that the clefts connecting this space to the bulk extracellular fluid are greatly expanded, according to electron micrographs. No value for the measured thickness of the space or of the clefts is given. From their data and discussion, it is probably

---

FIGURE 11. (*opposite*) Freeze-fracture replica of crayfish axon and surrounding glial cell connective tissue layers. The top surface of the schematic diagram shows the fracture plane. The diagram is drawn to scale in the vertical direction, but not in the horizontal direction. The tubule diameter is actually two to three times the thickness of the periaxonal space (see Fig. 10). A, axoplasm. P_{AX}, protoplasmic face of the axon membrane. E_{SC}, exoplasmic face of the Schwann cell membrane bordering the periaxonal space. SC, Schwann cell cytoplasm. P_{SC}, protoplasmic face of the outer Schwann cell surface. C, adjacent connective tissue layer. P, projections. Tubule openings are visible in the E_{SC} and P_{SC} surfaces (arrowheads). They appear as protrusions on E_{SC} and as dimples on P_{SC} because the fracture plane follows the tubular membrane for a few nanometers before crossing the tubule lumen (see diagram). The arrows indicate a tubule seen to traverse the Schwann cell. × 29,000.

not possible to eliminate rapid washout kinetics as a cause of the large apparent space.

On the other hand, the situation in squid nerve fibers seems quite distinct from that of both crayfish and *Myxicola*. As noted earlier, loading of the periaxonal space is well predicted from the total K^+ flux and the anatomically measured thickness and is consistent with slow washout kinetics (Frankenhaeuser and Hodgkin, 1956). The structure of the Schwann cells of squid giant axons has been studied by Geren and Schmitt (1954), Villegas and Villegas (1960), and Villegas (1969). The narrow space between axon and Schwann cell communicates with the bulk extracellular fluid via a series of tortuous clefts between regions of glial cell cytoplasm. It is difficult to judge the distance between cleft openings in the periaxonal space from the published micrographs since most show only one or two such sites. Wooding (in Keynes et al., 1975) has measured the average interval in one fiber to be 13 μm, and Taylor et al. (1980) used this value in computing the time course of dissipation of excess $[K^+]_o$ ($\tau \simeq 80$ ms). The length of the clefts can be estimated to be 3–10 μm, or about eight times the Schwann cell thickness. Taylor et al. (1980) used 5 μm in their fit.

The structure we have demonstrated in crayfish axons is quite different. Relatively thin layers of glial cytoplasm alternate with regions containing extracellular fluid and connective tissue. The innermost glial cell layer contains an extensive network of membranous tubules. Holtzman et al. (1970) have found a similar system in Schwann cells of lobster giant axons and have shown that peroxidase penetrates the tubular network from the external medium. If excess $[K^+]_o$ leaves the periaxonal space primarily by diffusion, then, because the time constant for the process is $\sim$2 ms and the diffusion coefficient for K^+ is $\sim 10^{-5}$ cm^2/s, the pathway must be no more than 1.4 μm. We suggest that the glial tubular system may represent the pathway for rapid diffusion of ions away from the periaxonal space. If Na^+ and K^+ channels are located preferentially in the neighborhood (i.e., within $\sim$0.5 μm) of the tubular openings into the periaxonal space, excess ions would be rapidly diluted in the tubular system volume and ultimately (in the case of a high degree of loading) in the relatively large connective tissue regions. $[K^+]_o$ will thus depend on the magnitude and time course of K^+ current in a complex fashion. Two related phenomena must be explained if this scheme is correct. A large fraction of the resistance in series with the membrane of giant axons has generally been ascribed to the Schwann cell layer. Tubular elements would provide a relatively low resistance access to ionic channels in nearby axolemma. However, the series resistance (R_s) in crayfish axons, measured in current-clamp or voltage-clamp experiments, is substantial, $\sim$6 Ω cm^2 (Shrager and Lo, 1982). We tested whether a significant fraction of the R_s was associated with individual Na^+ channels, e.g., as a diffusion-limiting polysaccharide segment. Comparing Na^+ channel gating kinetics under conditions in which the ionic current through individual channels is

varied, while the total membrane current is held constant, showed that no more than 10% of the R_s is associated with individual Na^+ channels (Shrager and Lo, 1982). Most of the remaining R_s may arise in regions of the Schwann cell sheath beyond the immediate vicinity of the axon surface. Current pathways through the cytoplasmic and connective tissue strata are not clear in these regions and may involve more restricted flow.

Another difficulty with this anatomical model rests in explaining the kinetics of Na^+ channel block by TTX. At a toxin concentration of 3 nM, equilibrium block is approached with a time constant of 8–10 min in crayfish axons (Shrager and Lo, unpublished data), somewhat lower than the value of ~20 min found for squid fibers (Keynes et al., 1975). From the rate constants and Q_{10} for TTX block in the node of Ranvier given by Schwartz et al. (1973), values closer to 3 min would be expected. The slow onset of block in the squid has been attributed to specific binding to the axon membrane and nonspecific binding to glial and axonal surfaces (Keynes et al., 1975; Taylor et al., 1980). A similar mechanism may explain the result in crayfish axons, but would probably depend primarily on nonspecific binding to glial membranes (Tang et al., 1979), e.g., within the tubular network. We have no direct evidence regarding this possibility, and it must remain speculative.

The accumulation of K^+ in the perineural space during a train of action potentials may have an important modulating influence on excitability in the nervous systems of many different species. Increased $[K^+]_o$ might depolarize a cell between spikes and increase the level of resting inactivation of Na^+ channels, thereby limiting the maximum burst frequency. We conclude from this work that crayfish axons possess a specialized system to allow an accelerated removal of excess $[K^+]_o$ that is absent or less fully developed in squid axons. If the ultrastructural model is correct, it suggests that in the crayfish, Na^+ and K^+ channels may be located preferentially in regions of the axon membrane with relatively unrestricted access to bulk extracellular fluid. This presents an interesting comparison with the situation in myelinated axons of vertebrates in which Na^+ channels may be localized at breaks between glial processes, the nodes of Ranvier (Ritchie and Rogart, 1977). On the other hand, K^+ channels may be present in the paranodal region, or even in internodal segments (Chiu, 1981).

We thank Dr. Ted Begenisich for reading an earlier version of this manuscript and for offering helpful suggestions. We thank Ms. Karen Vogt and Ms. Wendy Keck for word processing.

This work has been supported by grants NS17965, NS10500, and GM20113 from the National Institutes of Health.

Received for publication 20 September 1982 and in revised form 9 March 1983.

REFERENCES

Adam, G. 1973. The effect of potassium diffusion through Schwann cell layer on potassium conductance of the squid axon. *J. Membr. Biol.* 13:353–386.

Adelman, W. J., Jr., Y. Palti, and J. P. Senft. 1973. Potassium ion accumulation in a periaxonal space and its effect on the measurement of membrane potassium ion conductance. *J. Membr. Biol.* 13:387–410.

Armstrong, C. M., F. Bezanilla, and E. Rojas. 1973. Destruction of sodium conductance inactivation in squid axons perfused with pronase. *J. Gen. Physiol.* 62:375–391.

Armstrong, C. M., and L. Binstock. 1965. Anomalous rectification in the squid giant axon injected with tetraethylammonium chloride. *J. Gen. Physiol.* 48:859–872.

Ballinger, M. L., and G. D. Bittner. 1980. Ultrastructural studies of several medial giant and other CNS axons in crayfish. *Cell Tiss. Res.* 208:123–133.

Bezanilla, F., and C. M. Armstrong. 1977. Inactivation of the sodium channel. I. Sodium current experiments. *J. Gen. Physiol.* 70:549–566.

Binstock, L., and L. Goldman. 1971. Rectification in instantaneous potassium current-voltage relations in *Myxicola* giant axons. *J. Physiol. (Lond.).* 217:517–531.

Chiu, S. Y. 1981. The effects of acute demyelination on the ionic currents in frog internode. *Biophys. J.* 33:92*a*. (Abstr.)

Dubois, J. M. 1981*a*. Simultaneous changes in the equilibrium potential and potassium conductance in voltage clamped Ranvier node in the frog. *J. Physiol. (Lond.).* 318:279–295.

Dubois, J. M. 1981*b*. Evidence for the existence of three types potassium channels in the frog Ranvier node membrane. *J. Physiol. (Lond.).* 318:297–316.

Dubois, J. M., and C. Bergman. 1975. Potassium accumulation in the perinodal space of frog myelinated axons. *Pflügers Arch. Eur. J. Physiol.* 358:111–124.

Frankenhaeuser, B., and A. L. Hodgkin. 1956. The after-effects of impulses in the giant nerve fibres of *Loligo*. *J. Physiol. (Lond.).* 131:341–376.

Gardner-Medwin, A. R. 1981. Possible roles of vertebrate neuroglia in potassium dynamics, spreading depression and migrane. *J. Exp. Biol.* 95:111–127.

Geren, B. B., and F. O. Schmitt. 1954. The structure of the Schwann cell and its relation to the axon in certain invertebrate nerve fibers. *Proc. Natl. Acad. Sci. USA.* 40:863–870.

Goldman, D. E. 1943. Potential, impedance, and rectification in membranes. *J. Gen. Physiol.* 27:37–60.

Hille, B. 1973. Potassium channels in myelinated nerve. Selective permeability to small cations. *J. Gen. Physiol.* 61:669–686.

Hodgkin, A. L., and A. F. Huxley. 1952. A quantitative description of membrane current and its application to conduction and excitation in nerve. *J. Physiol. (Lond.).* 117:500–544.

Hodgkin, A. L., and B. Katz. 1949. The effect of sodium ions on the electrical activity of the giant axon of the squid. *J. Physiol. (Lond.).* 108:37–77.

Holtzman, E., A. R. Freeman, and L. A. Kashner. 1970. A cytochemical and electron microscope study of channels in the Schwann cells surrounding lobster giant axons. *J. Cell Biol.* 44:438–445.

Horn, R., M. S. Brodwick, and D. C. Eaton. 1980. Effect of protein cross-linking reagents on membrane currents of squid axon. *Am. J. Physiol.* 238(3):127–132.

Keynes, R. D., F. Bezanilla, E. Rojas, and R. E. Taylor. 1975. The rate of action of tetradotoxin on sodium conductance in the squid giant axon. *Phil. Trans. R. Soc. Lond. B Biol. Sci.* 270:365–375.

Kriz, N., E. Sykova, and L. Vyklicky. 1975. Extracellular potassium changes in the spinal cord of the cat and their relation to slow potentials, active transport, and impulse transmission. *J. Physiol. (Lond.).* 249:167–182.

Lo, M.-V. C., and P. Shrager. 1981. Block and inactivation of sodium channels in nerve by amino acid acid derivatives. I. Dependence on voltage and sodium concentration. *Biophys. J.* 35:31–43.

Meves, H., and Y. Pichon. 1975. Effects of 4-aminopyridine on potassium current in internally perfused giant axons of the squid. *J. Physiol. (Lond.).* 251:60P–62P.

Moran, N., Y. Palti, E. Levitan, and R. Stampfli. 1980. Potassium ion accumulation at the external surface of the nodal membrane in frog myelinated fibers. *Biophys. J.* 32:939–954.

Nicholson, C. 1980. Dynamics of the brain cell microenvironment. *Neurosci. Res. Prog. Bull.* 18:183–322.

Orkand, R. K. 1979. Extracellular potassium accumulation in the nervous system. *Fed. Proc.* 39:1515–1518.

Orkand, R. K., J. G. Nicholls, and S. W. Kuffler. 1966. Effect of nerve impulses on the membrane potential of glial cells in the central nervous system of amphibia. *J. Neurophysiol.* 29:788–806.

Peracchia, C. 1974. Excitable membrane ultrastructure. I. Freeze fracture of crayfish axons. *J. Cell Biol.* 61:107–122.

Peracchia, C., and J. D. Robertson. 1971. Increase in osmiophilia of axonal membranes of crayfish as a result of electrical stimulation, asphyxia, or treatment with reducing agents. *J. Cell Biol.* 51:223–239.

Ritchie, J. M., and R. B. Rogart. 1977. The density of sodium channels in mammalian myelinated nerve fibers and the nature of the axonal membrane under the myelin sheath. *Proc. Natl. Acad. Sci. USA.* 74:211–215.

Schwartz, J. R., W. Ulbricht, and H.-H. Wagner. 1973. The rate of action of tetrodotoxin on myelinated nerve fibers of *Xenopus laevis* and *Rana esculenta*. *J. Physiol. (Lond.).* 233:167–194.

Shrager, P. 1974. Ionic conductance changes in voltage-clamped crayfish axons at low pH. *J. Gen. Physiol.* 64:666–690.

Shrager, P. 1975. Specific chemical groups involved in the control of ionic conductance in nerve. *Ann. NY Acad. Sci.* 264:293–303.

Shrager, P., and M.-V. C. Lo. 1982. Influence of ionic current on Na^+ channel gating in crayfish giant axon. *Nature (Lond.).* 296:450–452.

Shrager, P. G., R. I. Macey, and A. Strickholm. 1969. Internal perfusion of crayfish giant axons: action of tannic acid, DDT and TEA. *J. Cell. Physiol.* 74:77–90.

Shrager, P., and J. G. Starkus. 1979. Block of sodium inactivation in nerve by polyphenols; ion accumulation in the Schwann cell space. *Biophys. J.* 25:306*a*. (Abstr.)

Starkus, J. G., and P. Shrager. 1978. Modification of slow sodium inactivation in nerve after internal perfusion with trypsin. *Am. J. Physiol.* 235(5):C238–C244.

Tang, C. M., G. R. Strichartz, and R. K. Orkand. 1979. Sodium channels in axons and glial cells of the optic nerve of *Necturus maculosa*. *J. Gen. Physiol.* 74:629–642.

Taylor, R. E., F. Bezanilla, and E. Rojas. 1980. Diffusion models for the squid axon Schwann cell layer. *Biophys. J.* 29:95–117.

Van Harreveld, A. 1936. A physiological solution for fresh water crustaceans. *Proc. Soc. Exp. Biol. Med.* 34:428–432.

Varon, S. S., and G. G. Somjen. 1979. Neuron-glia interactions. *Neurosci. Res. Prog. Bull.* 17:1–239.

Villegas, G. M. 1969. Electron microscopic study of the giant nerve fiber of the giant squid *Dosidicus gigas*. *J. Ultrastruct. Res.* 26:501–514.

Villegas, R., and G. M. Villegas. 1960. Characterization of the membranes in the giant nerve fiber of the squid. *J. Gen. Phsyiol.* 43:73–103.

Wallin, G. 1966. Simultaneous determination of membrane potential and intracellular ion concentrations in single nerve axons. *Nature (Lond.).* 212:521–522.

Yeh, J. Z., G. S. Oxford, C. H. Wu, and T. Narahashi. 1976. Interactions of aminopyridines with potassium channels of squid axon membranes. *Biophys. J.* 16:77–81.